Infrared Heating of Hydrogen Layers in Hohlraums

B. J. Kozioziemski, R. L. McEachern, R. A. London, D. N. Bittner

August 21, 2001

U.S. Department of Energy

Lawrence
Livermore
National
Laboratory

Infrared heating of hydrogen layers in hohlraums

B. J. Kozioziemski, Randall L. McEachern, and R. A. London

Lawrence Livermore National Laboratory, Livermore CA 94551

D. N. Bittner

Schafer Corporation 303 Lindbergh Ave. Livermore CA 94550

(Dated: June 24, 2003)

We report results of modeling and experiments on infrared heated deuterium-hydride (HD) layers in hohlraums. A 2 mm diameter, 40 μm thick shell with 100-400 μm thick HD ice inside a NIF scale gold hohlraum is heated by pumping the HD vibrational-rotational bands. Models indicate control of the low-mode layer shape by adjusting the infrared distribution along the hohlraum walls. We have experimentally demonstrated control of the layer symmetry perpendicular to the hohlraum axis.

I. INTRODUCTION

Smooth, uniformly thick 50-300 μm thick deuterium-tritium (D-T) layers inside 1 to 3 mm diameter spherical capsules are required for ignitable inertial confinement fusion (ICF) targets for the National Ignition Facility (NIF). Smooth (< 1 μm rms) D-T layers are formed by slowly cooling the liquid through the melting point, with the solid phase starting from a single seed crystal[1]. The tritium beta-decay heats the solid, causing the high vapor pressure ice to re-distribute itself inside the capsule to minimize its thermal energy. Thickness peturbations in the layer decay exponentially with a time constant of $\tau = 27$ minutes[2,3]. This process culminates in an ice layer with an isothermal surface. Crystal facets and grain boundaries prevent the native beta-layering from smoothing out small scale defects[1,4]. The thermal gradient across the ice, the driving force for re-distribution, is increased by pumping the collisionally induced infrared (IR) vibration-rotation band, allowing faster redistribution, smoother layers, and lower temperatures[5]. Additionally, smooth layers of the non-radioactive hydrogen isotopes (D_2, HD) used in non-ignition hydrodynamic experiments can be produced using infrared heating.

Our previous experiments achieved a highly uniform temperature profile in a spherical ice layer by centering the capsule inside a spherical cavity[1,6]. Beta-layered D-T takes the shape of the spherical isotherms to minimize the thermal energy, producing ice layers with about 1.2 μm rms surface roughness. IR heating experiments using HD were performed with the capsule centered in an infrared integrating sphere, to symmetrically distribute the IR[6].

The baseline indirect drive target design consists of a 2 mm diameter capsule centered inside a cylindrical hohlraum 9.5 mm long and 5.5 mm diameter[7]. The gold hohlraum walls are isothermal, so a uniformly heated ice layer is subjected to non-spherical isotherms. Figure 1 shows the isotherms and temperature on the inner surface of a uniform, spherical ice layer for a D-T capsule inside a constant temperature hohlraum. The ice is forced to be symmetric by the calculation, however, in reality it moves in response to the isotherms and the resulting layer
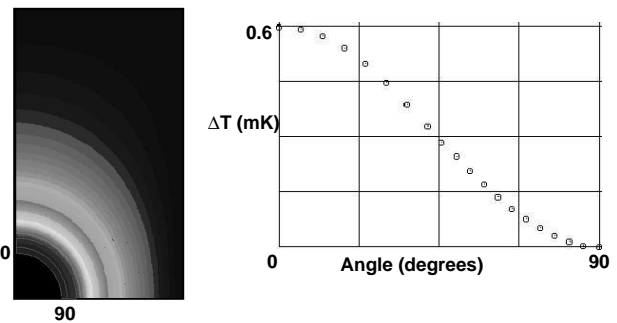

FIG. 1: The isotherms for a beta-decay heated D-T filled capsule inside a cylindrical hohlraum are shown on the left. The temperature difference along the inner surface of the D-T ice is plotted on the right as a function of angular position.

will not be spherically symmetric. Rather, the ice is thinner at the pole ($\theta = 0°$) than at the equator ($\theta = 90°$). The inner ice surface is conveniently described by Legendre modes of the angular variable θ, with the l=2 mode (P_2) dominating for this geometry. Our first goal is to inject the IR into the hohlraum and heat the capsule in a manner that minimizes P_2.

A computer model was developed to explore various IR illumination geometries. A suitable illumination geometry was found that allows for control of P_2 by moving the optics axially relative to the hohlraum. We have undertaken experiments to test the model and provide confidence in designing the NIF cryogenic target system. The raytrace and thermal model calculations are described in section II and the experimental results are presented in section III.

II. RAYTRACE AND THERMAL MODELS

Our modeling effort consists of two parts. We use the raytracing program TracePro[8] to compute the IR power absorbed in the capsule, ice, and hohlraum walls. The resulting heating data is then used as imput in the COSMOS[9] finite element program to find the temperatures in the ice, capsule, and hohlraum. The raytrace
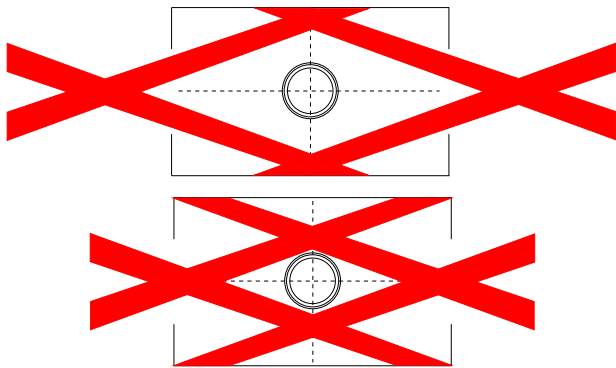
FIG. 2: Infrared illumination in a hohlraum for P2 control. The top and bottom are the two extreme pointing cases, at the center of the hohlraum and toward the end-caps, respectively. Pointing at the center of the hohlraum makes the shell equator hot, while pointing toward the LEH makes the poles hot. Each is rotationally symmetric about the hohlraum axis. IR is incident on the hohlraum wall at about $70°$ to the normal.
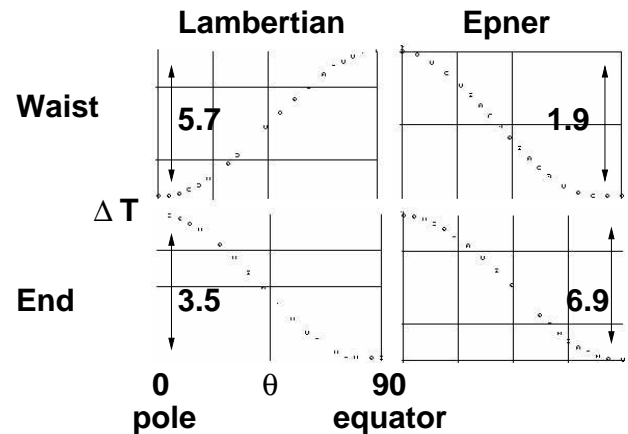

FIG. 3: Temperature variation around the inner ice surface for two different scattering surfaces and laser pointing. The sign change of the temperature difference from pole to equator between the end and waist pointing indicates the ability to zero P_2 for a Lambertian surface. The S_1 surface cannot produce a zero P_2 simply by adjusting pointing.

model itself is 3D, but the imposed azimuthal symmetry reduces the thermal analysis to 2D. The model reflects the current experimental configuration, a 10 mm long, 6 mm diameter gold hohlraum with 3 mm diameter laser entrance holes (LEH). A 2 mm diameter, 40 μm thick deuterated-plasma polymer capsule containing a 150 μm thick layer of ice is centered in the hohlraum. The hohlraum and shell are enclosed in a copper can connected to the cold tip of a liquid helium flow cryostat, and cooled by 1 torr of helium exchange gas in the can. Convective effects are minimized with this low helium density. The ice properties used were those of D_2: the absorption coefficient $\alpha_i = 0.4$ mm^{-1} at 3.16 μm and the index of refraction $n_i = 1.15$. For the plastic shell $\alpha_s = 0.1$ mm^{-1} and $n_s = 1.5$. The optical properties of HD are nearly the same as D_2 except that $\alpha_i = 0.8$ mm^{-1} at 2.57 μm.

Integrating sphere experiments demonstrated that direct illumination of the capsule by the laser must be avoided. Instead, the laser light is injected through the LEH as a hollow cone that illuminates a band around the cylindrical hohlraum wall. This geometry, shown in figure 2, avoids hitting the shell on the first pass and provides cylindrically symmetric illumination. In addition, the hohlraum wall must be a diffusely scattering surface to produce nearly uniform illumination. The TracePro simulation uses a parameterization of the bidirectional reflectance distribution function (BRDF) to model scattering at surfaces. An ideal Lambertian scatter has a constant BRDF, the light is scattered into a cosine distribution independent of incident angle. For real surfaces, the scattering behavior must be measured. Two roughened hohlraum surfaces were characterized for modeling purposes. Both were made by sand-blasting a copper mandrel, overcoating it with gold, then leaching out the copper. The rougher of the two (S_1) had an rms roughness (R_q) of 3 μm, compared with 1 μm for the smoother surface (S_2). These surfaces scatter well for near normal incidence, but are increasingly specular approaching grazing incidence, with the smoother sample more specular. The initial runs used the nearly ideal gold reflectivity of 96%, while later runs used the experimentally measured value of 65%. The peak power absorbed in the ice is set to $Q_{IR} = 5.0 \times 10^5$ W/m^3, 10 times the D-T beta-decay heating. The laser position, incident angle, and surface scattering function were varied in the model to determine their effect on the ice temperature profile. Normally, illumination through one LEH was modeled and the absorption data reflected about the equator to take into account illumination from both sides. In these cases P_1 is eliminated and P_2 is the dominant mode.

The hohlraum geometry presents two extremes for axial placement of the IR, near the equator of the hohlraum and near the LEH. Since the equator is the coldest part of the ice layer, extra heating needs to be applied there to counteract the intrinsic P_2. The model results are shown in figure 3. The temperature difference between the pole and equator of the ice layer changes sign when the Lambertian surface is used, whereas for the S_1 surface the equator is still relatively colder, even when the IR is injected at the equator. Therefore, the magnitude of P_2 can be reduced to near zero with a Lambertian scattering surface, but not with the S_1 or S_2 surfaces.

The above model, using a surface with 96% reflectivity, predicts that 7.0% of the light entering the hohlraum is absorbed by the ice, with a temperature drop from the ice to the cryostat cold tip of about 3 K. As described in the experimental section, these predictions differed significantly from the experiment. The model was re-run with the measured reflectivity of 65%. In this case we do find the P_2 can be zeroed out with an S_1 hohlraum surface by moving the IR along the hohlraum wall. Further,

the ice absorbs only 2% of the IR entering the hohlraum, much closer to the value measured by the ice redistribution time constant, and the temperature drop from the ice to the cold tip is consistent with the experiment.

A. One sided illumination

The experiments to date have used illumination from one side only. This introduces a substantial P_1 component to the ice layer. One sided illumination is modeled by running TracePro and COSMOS with a P_1 defect introduced in the ice layer and varying the P_1 amplitude until the temperature variation along the inner ice surface is minimized. Figure 4 shows the result for a Lambertian surface with 4% absorption and 10 Q_{DT} IR heating. The large temperature variation for a centered ice layer is substantially reduced when a P_1 value 10% of the ice layer thickness is introduced. The optical properties of the ice are responsible for a 10% effect in the P_1 magnitude, as determined by using the $P_1 = 0$ raytrace heating data with the $P_1 = 15$ μm thermal model. The P_1 amplitude could not be measured in the current experiment, but upcoming experiments will include this capability.

III. EXPERIMENTS

The experiment was undertaken to provide feedback to the model and give confidence in its predictions. The illumination was limited to one side to simplify initial alignment of the optics to the hohlraum and understand the response of the layer to movement of the IR beam along the wall.

A. Experimental setup

The optical system had to satisfy several requirements. First, a ring of IR light needed to be projected onto the hohlraum wall as described by the model. Second, accommodation of optical imaging of the capsule along the hohlraum axis was required for data collection. Finally, the IR had to be accurately positioned with respect to the hohlraum.

The reflective optical system shown in figure 5 was designed with the above requirements taken into account and provided many benefits over refractive optics. The wavelength independence allows a HeNe ($\lambda = 0.633$ μm) laser to be used for initial alignment. The main reflector (M_1) was made large enough to accommodate both the low f/# used for the IR illumination and a turning mirror (M_2) for imaging the target at f/3. The surface of M_1 is defined by an arc of a circle revolved around the symmetry axis. The slight curvature focuses the light through the LEH and onto a 2 mm length of the hohlraum wall. The curvature also allows the injection angle to be varied between 65° and 75° from the wall normal.
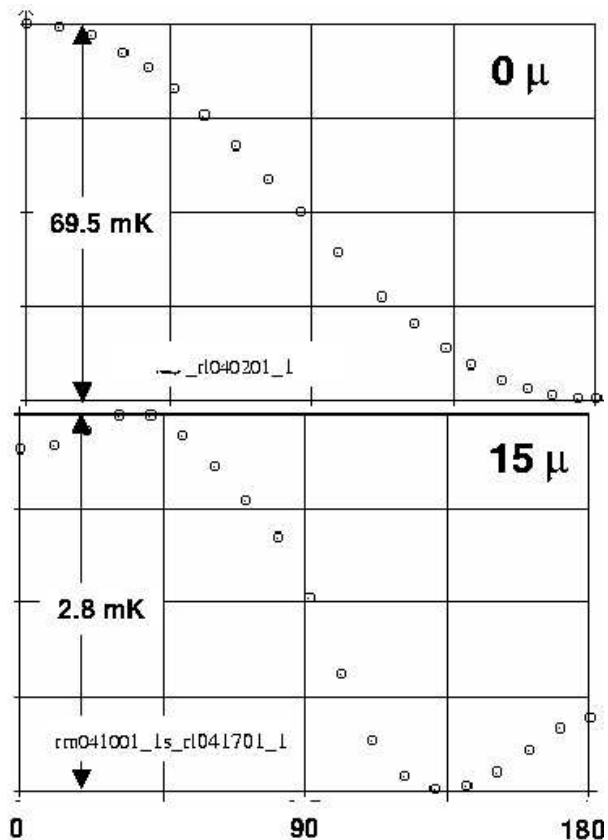
FIG. 4: Temperature variation around the ice layer using 1 sided illumination and S_1 hohlraum surface. The top figure is the temperature on the inner ice surface for a centered ice layer, while the bottom figure is that when the ice layer is moved off by 15 μm.

The lasers are fiber coupled, with the fiber output collimated by a parabolic mirror, enabling simple switching between laser sources. The approximately 5 mm diameter collimated beam is reflected by the 45°, 10 mm base diameter conical mirror (M_c) onto M_1. The position of M_c relative to M_1 selects the angle of the beam on the hohlraum wall. The cone described by the light is large enough to pass around a 1 inch turning mirror (M_2) before entering the hohlraum. A laser power meter was periodically inserted between the parabolic mirror and M_c to record the power. The power into the hohlraum was calculated based on an initial reference measurement made by placing the power meter at the hohlraum position.

Correct alignment of the optical elements relative to each other was obtained using visible light from the HeNe laser to observe the propagated beam shape through the optics. We start by rotating M_c relative to M_1 until a circular beam is observed. The collimated beam is centered on M_c when the circle has uniform intensity. A 0.5 mm diameter hole in the center of M_c passes a small amount of the collimated light which serves as the reference for the center of the circular beam. The entire optical system
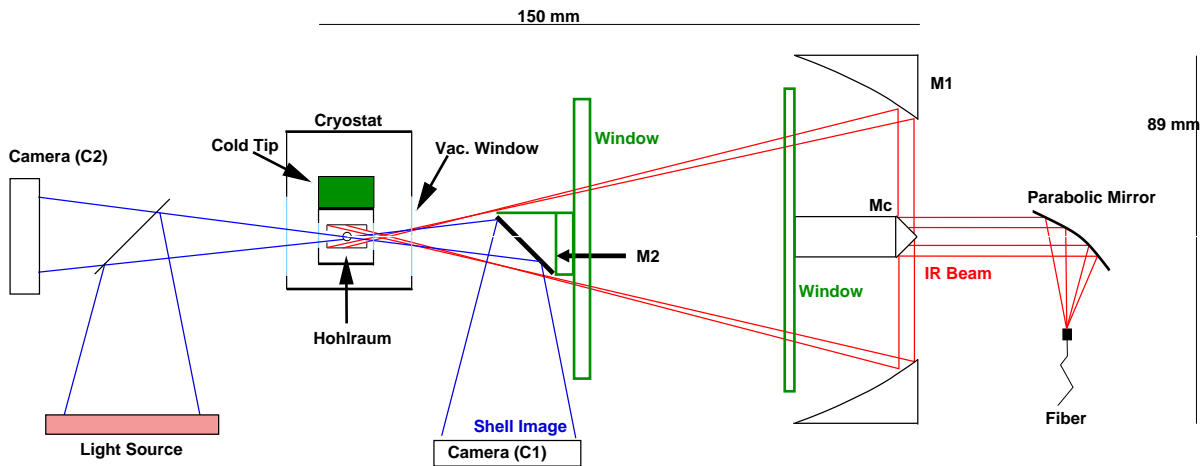
FIG. 5: Reflective optical system for IR heating of HD ice inside a hohlraum. A ring of light is projected onto the hohlraum wall using a 45° conic mirror (M_c)and a large cylindrical mirror (M_1). A small turning mirror (M_2) is placed inside the large ring to view the shell while layering.

is positioned with a 5-axis stage so the reference beam passes through the center of the shell. The assembly is moved so the ring of light just passes through the LEH and marks z = 0 for the system.

One additional alignment aid was discovered during the experiments. Visible laser light reflected from the ice-vapor and the shell-ice interfaces was recorded by camera C_2. The imaged light indicates the uniformity of the injected light in the hohlraum and proved to be very sensitive to misalignments of the optics relative to each other and the hohlraum. Fine adjustments to the optics were made to produce a uniform intensity circle on C_2. Furthermore, the IR lasers have small amounts of visible light co-propagating with the IR, enabling us to adjust the IR in real-time. Two examples are show in figures 6 and 7. The first shows the image when small misalignments exist in the optical system. The second shows the image obtained after correcting the optics. The bright ring has an apparent radius of 875 μm, compared to the shadowgraph image 600 μm for the inner ice surface.

The hohlraum and shell are described in section II. The S_1 gold surface was used. An Aculight model 1100 optical parametric oscillator (OPO) laser and a Burleigh F-center laser were alternately used to illuminate the hohlraum. HD was used in these experiments because it has higher absorption than D_2 and the F-center laser output is higher for the HD line ($\lambda = 2.57$ μm) than the D_2 line ($\lambda = 3.16$ μm). The IR power into the hohlraum was typically between 9 and 13 mW and was limited by the heat extraction through the helium exchange gas.

The target was backlit through the LEH and imaged with a Questar QM 100 long working distance microscope onto a Photometrics CCD camera (C1), as illustrated in figure 2. The camera has a 1317x1035 pixel, 12 bit chip. The object resolution is 2.5 μm/pixel with the shell image nearly filling the chip. A real time video camera (C2) viewing through the second LEH was used with the
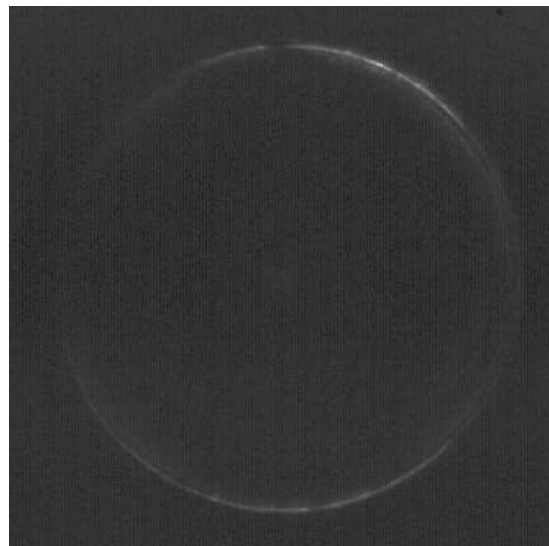

FIG. 6: Image on camera C_2. The light reflected from the shell is not uniform and indicates the optics are not well aligned to the hohlraum. The image width is 2 mm.

HeNe to provide precise alignment of the injection optics to the hohlraum.

Germanium resistance thermometers record the temperature at the cold tip and are used for temperature control. The IR heating creates a substantial temperature drop between the ice layer and the cryostat cold tip, as determined by the ice melting temperature.

B. Layering

Our initial experiments tested the cylindrical symmetry of a layer formed in hohlraums. Only single sided illumination and shadowgraphy were required to perform
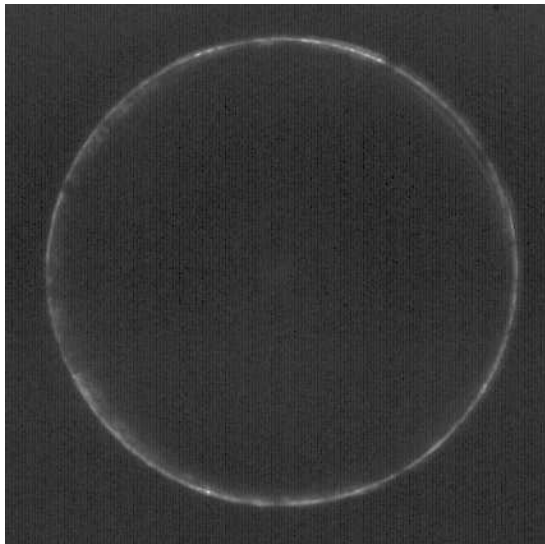
FIG. 7: Image on camera C_2. The uniform reflection from the shell indicates the optics are well aligned to the hohlraum. The image width is 2 mm.

FIG. 8: The HD ice before IR layering. The ice moved to the relatively cooler center of the shell overnight due to room light entering the hohlraum. The ice returned to nearly the same shape every night.
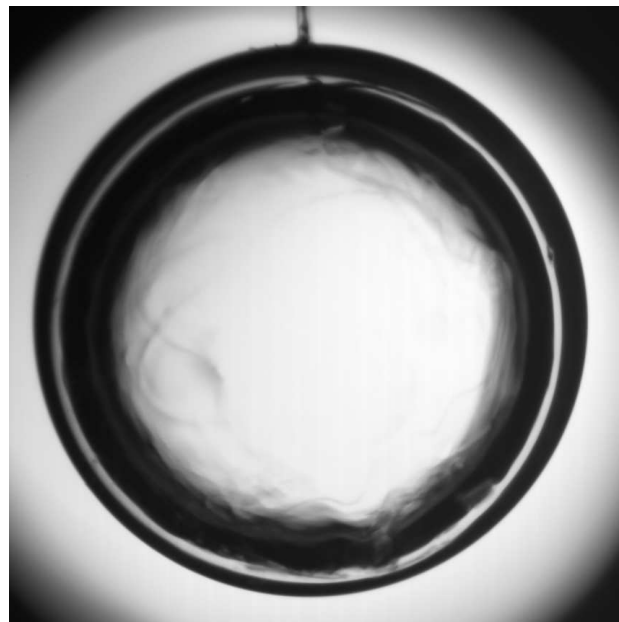

FIG. 9: The ice in figure 8 has been heated by 9 mW IR injected into the hohlraum and layered for 2 hours. The layer has very good symmetry.

these experiments. The layers were typically formed either by cooling HD through its freezing temperature or by starting from the solid. Both methods produced similar results, but the solid redistribution time constant τ was more easily measured when starting from the liquid phase. In this case, the layer starts thin at the top of the shell and approaches the steady state thickness exponentially with a rate inversely proportional to the volumetric heating[2,3].

Figure 8 shows the HD ice before IR layering. When left overnight, the ice migrates away from the LEH to the equator of the shell, where the temperature is slightly lower. The ice is then heated without melting by 9 mW of IR. It evolves continuously over two hours to reach the nearly steady state shown in figure 9. The bright band, which follows the inner ice surface[6], indicates that the layer has a number of defects but overall has very good azimuthal symmetry.

The IR distribution inside the hohlraum controls the azimuthal layer shape. Figure 10 shows the layer response to intensity changes in the IR. The top left image shows the initial layer before IR is applied. The top right shows the layer formed by 10 mW of IR heating when the applied IR ring is uniform. Large crystal facets are apparent in the image due to the rapid crystal growth during layering, but the ice shape is well centered in the shell. The optics are then deliberately misaligned so the IR intensity is higher on the left side than the right, producing the ice configuration in the bottom left image. Finally, the optics are returned to their original position and a symmetric ice layer is regained.

The sensitivity of the ice layer to misalignments of the injection optics was tested by recording the ice layer as the optics were moved. The response of the ice layer to horizontal movement of the optics is shown in figure

11. The laser power was 12 mW into the hohlraum and the helium exchange gas pressure was 100 torr. The layer starts with a 32 μm lateral offset at x = 0 due to imperfect initial alignment. When the stage is moved to x = 152 μm at t = 100 minutes, the lateral offset increases to 41 μm. When the stage is moved to x = -102 μm, the offset is reduced to about 25 μm. In both cases the ice approaches a steady state value with an exponential rate.
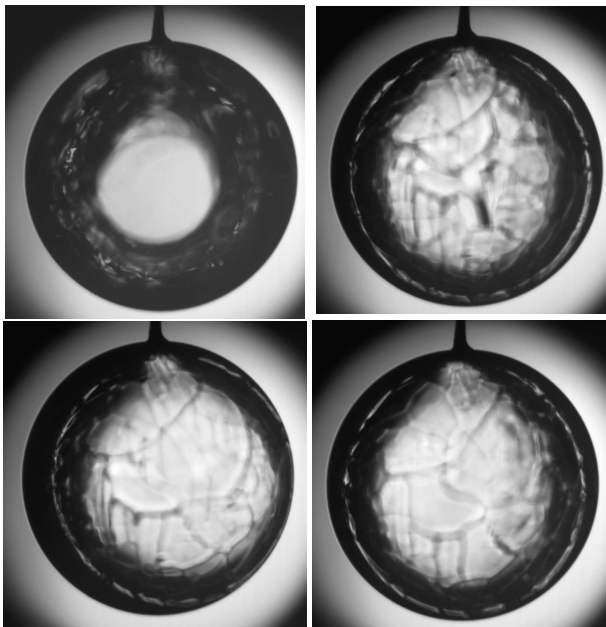
FIG. 10: This series of images shows the ice response to misalignment of the optics. The initial ice shape (top left) is redistributed by IR heating to a more uniform shape (top right). The IR optics are misaligned so the ring has higher intensity on the right side than the left, forcing the ice to move (bottom left). When the optics are returned to the original position, the ice returns to its initial shape (bottom right).
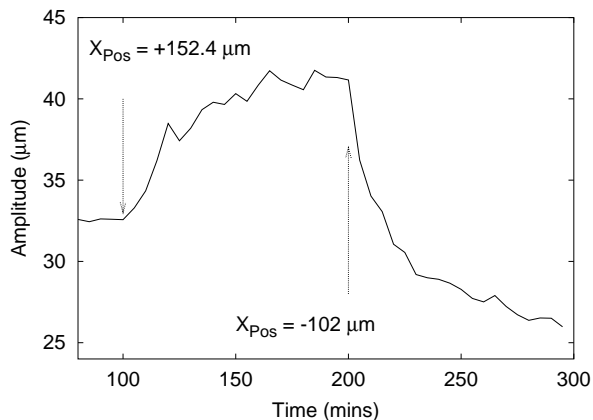

FIG. 11: The misalignment of the IR optics relative to the hohlraum forces the layer to move. The lateral offset is shown as a function of time. At 100 minutes, the optics were moved horizontally to x = 152 μm and the offset increases. At 200 minutes the optics are moved to x = -102 μm and a corresponding decrease in the amplitude is observed.

The redistribution time constant was measured to determine the volumetric heating of the ice. The time constant was most easily measured by cooling the HD liquid through the triple point under IR illumination. Most of the liquid freezes at the bottom of the shell, and the thickness increase near the top of the shell is easily measured
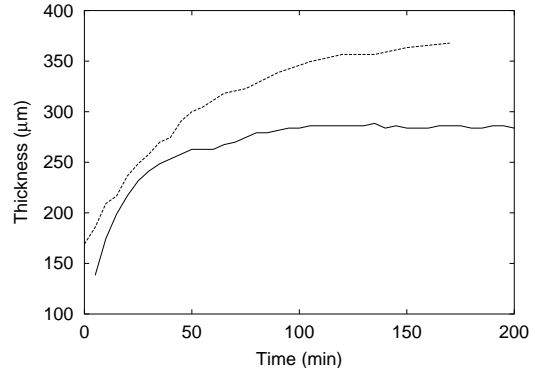

FIG. 12: Measured thickness of HD ice as a function of time. The solid line is 1.4 K below the melting temperature with 9 mW of IR entering the hohlraum, while the dashed is for ice 1.1 K below T_m and 3 mW IR.

by recording images at a given time interval. Figure 12 shows two time constant measurements. The solid line is for HD 1.4 K below its melting point with 9 mW of IR, while the dashed line is for 1.1 K below melting and 3 mW of IR. The time constants are 20 and 52 minutes for the 9 mW and 3 mW IR powers respectively. The time constant is inversely proportional to the heating rate, as expected. The 20 minute time constant corresponds to a bulk heating of 1.3 Q_{DT}. This is still lower than the value of 2.4 Q_{DT} predicted by the models, but is much closer than the 8.5 Q_{DT} value using the 96 % reflectivity value.

IV. CONCLUSIONS

A computational model was developed to study illumination methods for heating a spherical ICF target inside a cylindrical hohlraum. Our baseline design uses the position of the IR illumination in the hohlraum to remove the P_2 asymmetry of the ice layer. Experiments to test the validity of the model have produced qualitative agreement and led to some refinements of the model. Future experiments will improve on the current experiment and diagnostics to enable a more precise comparison between the model and experiment.

Acknowledgments

[1] J. Sater, B. Kozioziemski, G. W. Collins, E. R. Mapoles, J. Pipes, J. Burmann, and T. P. Bernat, Fusion Technology **35**, 229 (1999).

[2] A. J. Martin, R. J. Simms, and R. B. Jacobs, J. Vac. Sci. Technol. A **6**, 1885 (1988).

[3] J. K. Hoffer, L. R. Foreman, J. J. Sanchez, E. R. Mapoles, and J. D. Sheliak, Fusion Tech. **30**, 529 (1996).

[4] G. W. Collins, T. P. Bernat, E. R. Mapoles, and B. J. Kozioziemski, Phys. Rev. B. **63**, 195416 (2001).

[5] G. W. Collins, D. N. Bittner, E. Monsler, S. Letts, E. R. Mapoles, and T. P. Bernat, J. Vac Sci. Technol. A **14**, 2897 (1996).

[6] D. N. Bittner, G. W. Collins, E. Monsler, and S. Letts, Fusion Tech. **35**, 244 (1999).

[7] J. Lindl, Physics of Plasmas **2**, 3933 (1995).

[8] Raytracing was performed using the TracePro^{TM} commercial optical modeling program. For further information contact Lambda Research Corp., Littleton, MA 01460.

[9] Thermal modeling was performed using the COSMOS commercial finite element method program. For further information contact Structural Research & Analysis Corp. Los Angeles, CA 90025.